ISSN 1330-3651 (Print), ISSN 1848-6339 (Online)
https://doi.org/10.17559/TV-20250210002358
Original scientific paper

The Effect of Composition and Heat Treatment on Impact Toughness of Hadfield Steel

Aleksandar VUKOSAVLJEVIĆ, Aleksandar SEDMAK*, Srđan TADIĆ, Srđa PERKOVIĆ, Nenad RADOVIĆ

Abstract: The effect of composition and heat treatment on impact toughness of Hadfield steel is investigated. Water quenching and additional aging was applied to 12Mn steel (two different compositions), 16Mn and 16MnV steels and instrumented Charpy pendulum is used to determine the total energy, as well as the energies for crack initiation and propagation to follow closely the effects of composition and heat treatment. Microstructure was examined as well, to get better insight into these effects. It was shown that 16Mn steels after water quenching and 12Mn steels after water quenching and aging have satisfactory impact toughness values. In any case, steels investigated here turned out to be sensitive to cracking, whereas their resistance to crack propagation was good enough.

Keywords: crack initiation energy; crack propagation energy; hadfield steel; impact toughness; water quenching and aging

1 INTRODUCTION

Sir Robert Abbott Hadfield discovered Manganese steel, back in 1882, one of the first alloy steels. His invention was based on adding a large amount of manganese to molten steel, thus producing steel with high strength and hardness, among other excellent characteristics [1]. He concluded that the optimal strength and hardness can be reached with Mn content between 11-13 % and Carbon content between 1-1.3 %, with Mn/C ratio of 10:1, [1].

A unique property of this high-strength steel is strain hardening from a yield strength of cca 400 MPa to a maximum tensile strength of nearly 1000 MPa. During the abrasive test, Hadfield steel performs better than forged alloy steels, cast alloy steels, stainless steels, tool steels or steels with a high chromium content. This is due to transformation of the austenite microstructure into a martensite caused by cold deformation under impact loading in the shallow subsurface layers [2-4]. At the same time, its capability to plastically deform is significantly reduced, making Hadfield steel sensitive to cracking [5].

Hadfield Manganese steel is capable of strain hardening, so it has been widely used in various fields such as railway construction, excavator parts, crusher segments and machine parts that must be resistant to wear and abrasion, [6] since it often has superior properties compared to other options, [7-8]. The mechanism of deformation strengthening is quite complex and has several interpretations, [3, 4]. Through this paper, based on metallographic and mechanical analyses of the samples, an attempt will be made to answer these interpretations.

In the as-cast state, Hadfield steel contains carbides that reduce its toughness and ductility, due to presence of dendrites. To obtain very fine carbides alloying elements that have a high affinity for C are added, like Cr and V, [6]. Such micrograph is shown in Fig. 1, with arrows marking carbides.

The dissolution treatment is used to remove unwanted carbides, at temperatures of 1000 °C and 1100 °C, with a dissolution time according to the size of parts. Casting and quenching temperatures have a large effect on the austenite grain size and final product properties. Other factors that determine the final properties of product are the chemical composition of casting, as well as the heat treatment. Therefore, different parameters, such as the content of alloying elements, casting conditions, quenching, micro-alloying elements and thermal cycles on castings determine the final microstructure [9].

In this paper the effect of composition and heat treatment on impact toughness of Hadfield steel is investigated. To do so heat treatment is required, consisting here of water quenching and additional aging applied to 12Mn (two slightly different compositions), 16Mn and 16MnV steels. Keeping in mind the importance of impact toughness for application of Hadfield steel, instrumented Charpy pendulum is used to determine not only the total energy, but also the energies for crack initiation and propagation, [10-13].

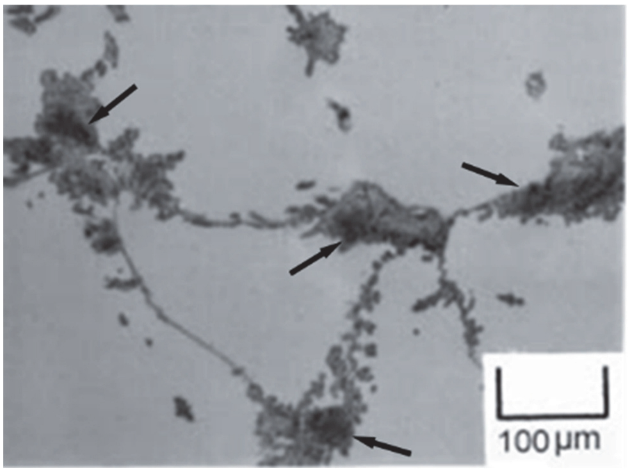

Figure 1 Microstructure of Hadfield steel with carbides on grain boundaries, [9]

2 MATERIALS AND METHODS

To perform the experimental Mn steel samples were prepared in industrial conditions (melting in a furnace, casting in a mould, heat treatment and making specimens Charpy impact toughness testing).

To analyse the effects of chemical composition and heat treatment, four alloys with varied chemical composition were tested. The first two alloys were from the Mn12, with different chemical composition of alloying elements, shown in Tab. 1. The other two alloys were from the Mn16, with different chemical composition, also shown in Tab. 1. All 4 alloys were treated with two heat treatments: the first, water quenching (WQ) after dissolution at 1050 °C, and the second one, water quenching and subsequent aging (WQA) for 2 hours, at 500 °C.

The following text samples (1)-(4) account for WQ heat treatment of 2 Mn12, Mn16 and Mn16V alloys, respectively, whereas their counterparts for WQA are marked as samples (5)-(8).

Table 1 Chemical analysis of 4 samples

Steel	C	Si	Mn	P	S	Cr	Ni	Mo	V
Mn12	1.02	1.11	11.32	0.06	0.009	1.58	0.285	0.083	-
Mn12	0.92	1.34	10.86	0.053	0.010	1.92	0.239	0.069	-
Mn16	1.08	0.60	14.11	0.059	0.002	2.40	0.149	0.043	-
Mn16V	1.18	0.60	14.49	0.043	0.001	2.05	0.044	0.015	0.475

2.1 Charpy Impact Toughness

Standard Charpy V notched specimens were used, Fig. 2, to determine the total impact energy, as well as energies for crack initiation and propagation on an instrumented Charpy pendulum. This is of high importance to know since it enables better understanding of material behaviour in presence of cracks [10-13]. Testing was conducted according to [14] at room temperature, using 3 specimens for each material and its specific state after heat treatment.

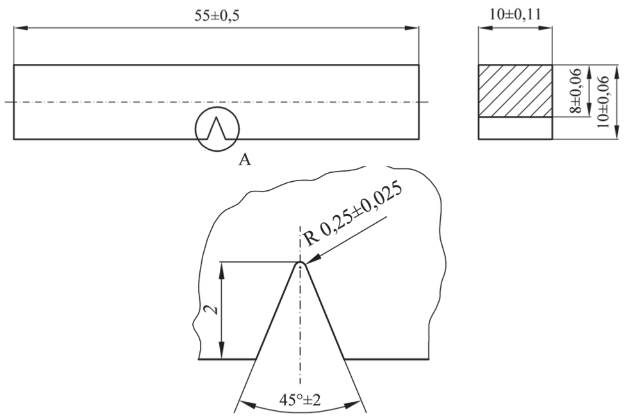

Figure 2 Standard Charpy ISO-V specimen with a notch in the center

3 RESULTSAND DISCUSSION

3.1 Microstructure

In respect to WQ treatment, typical microstructures of Mn12 sample (1) are shown in Figs. 3a-b, whereas Mn12 sample (2) is presented in Fig. 3c-d. In the case of Mn12 sample (1), the microstructure consists of austenite base and carbides at the grain boundaries and inside the grains, Fig. 3a-b. Similar to that is the microstructure of Mn12 samples (2), but with more pronounced carbides, Fig. 3c-d. In all figures black arrows indicate carbides.

In the case of WQ treatment, typical microstructures of Mn16 sample (3) are shown in Fis. 4a-b, whereas Mn16V sample (4) is presented in Fig. 4c-d. In the case of Mn16 sample (3), the microstructure consists of austenite base and carbides inside the base, Fig. 4a-b. Similar to that is the microstructure of Mn16V, sample (4), but with more pronounced carbides, Fig. 4c-d.

In respect to WQA treatment, typical microstructures of Mn12 sample (5) are shown in Figs. 5a-b, whereas Mn12 sample (6) is presented in Fig. 5c-d. In the case of Mn12 sample (5), the microstructure consists of austenite base and carbides at the grain boundaries and inside the base, Fig. 5a-b. Similar to that is the microstructure of Mn12 samples (6), but with more pronounced carbides, Fig. 5c-d.

In the case of WQA treatment, typical microstructures of Mn16 sample (7) are shown in Figs. 6a-b, whereas Mn16V sample (8) is presented in Fig. 6c-d. In the case of Mn16 sample (7), the microstructure consists of austenite base and carbides inside the base, Fig. 6a-b. Similar to that is the microstructure of Mn16V sample (8), but with more pronounced carbides, Fig. 6c-d.

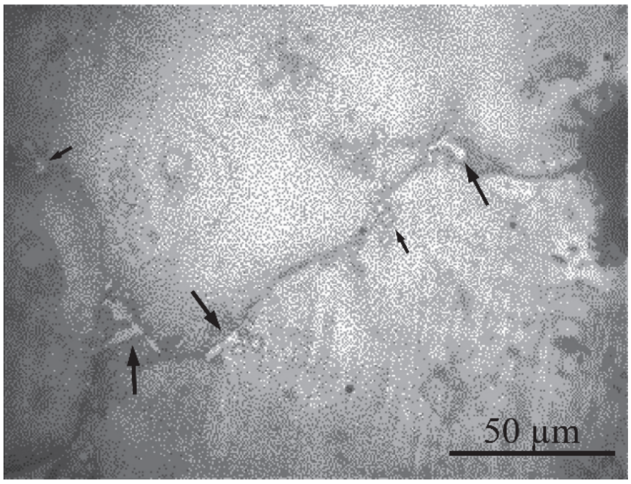

a)

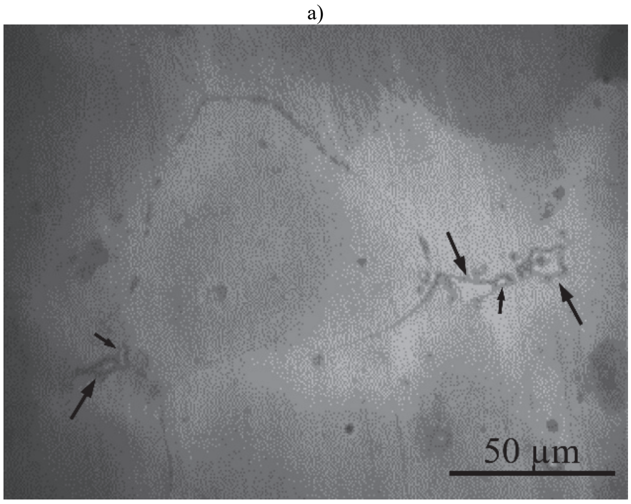

b)

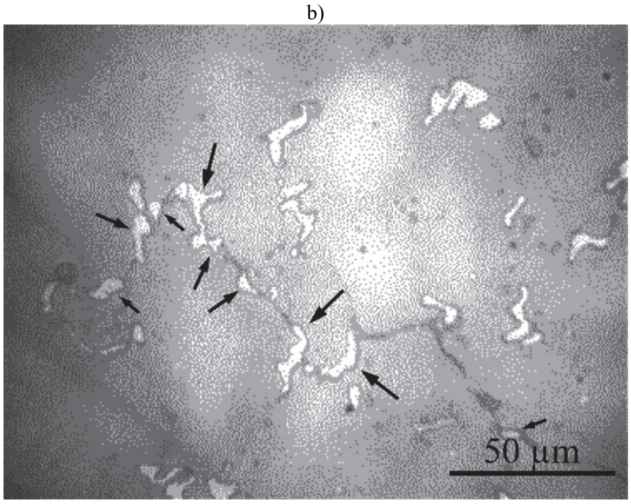

c)

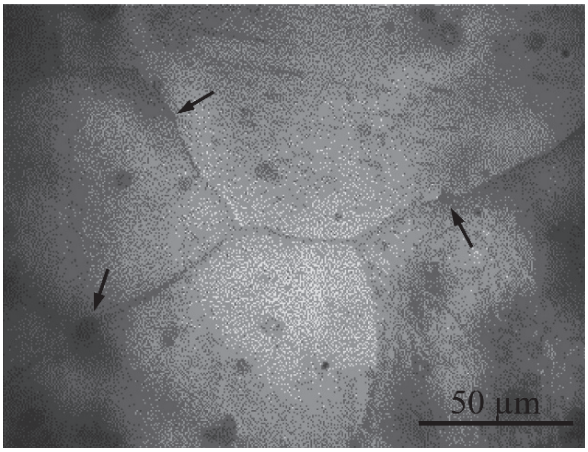

d)

Figure 3 Microstructure of Mn12 steel, WQ: a-b) sample (1); c-d) sample (2), magnification ×530, black arrows indicate carbides

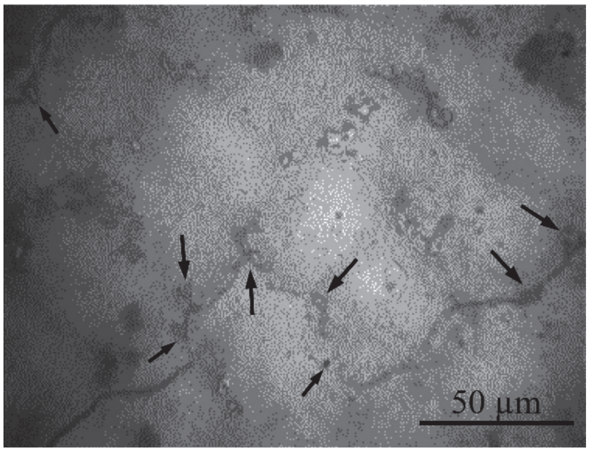

d)

Figure 4 Microstructure of Mn16 steel, WQ: a-b) sample (3); c-d) sample (4), magnification ×530, black arrows indicate carbides

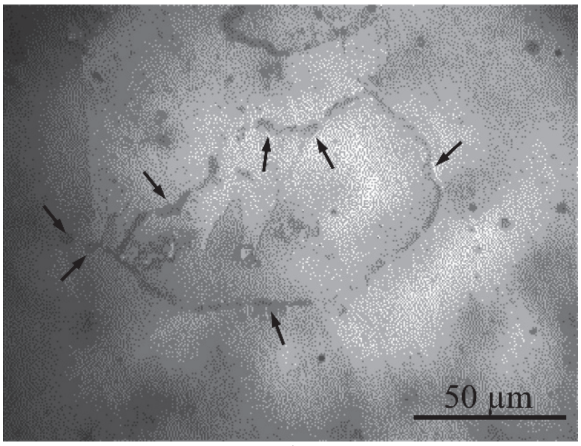

a)

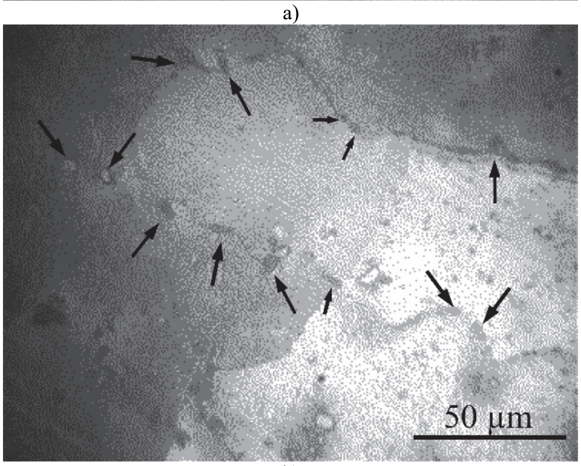

b)

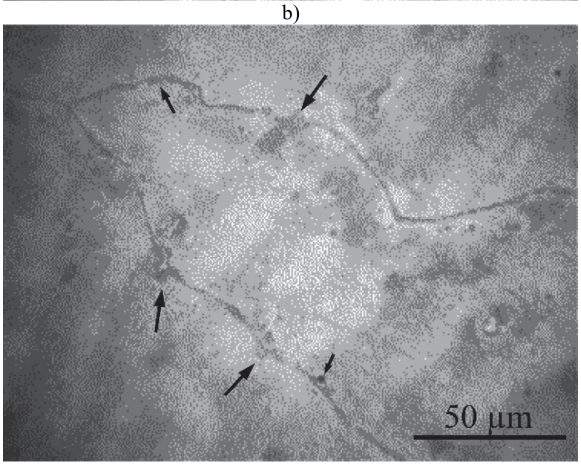

c)

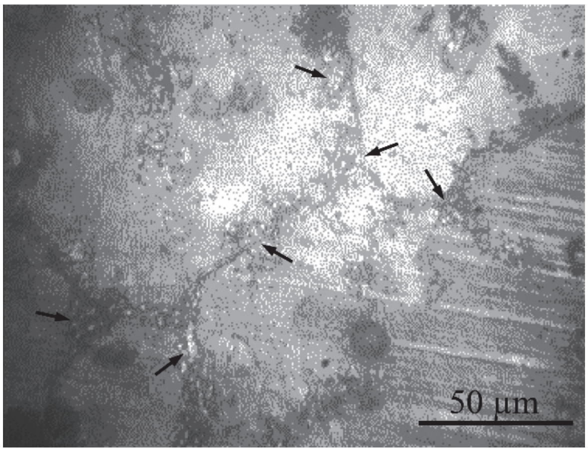

a)

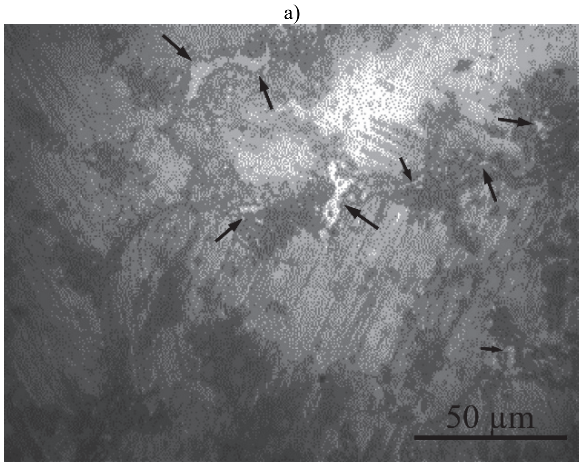

b)

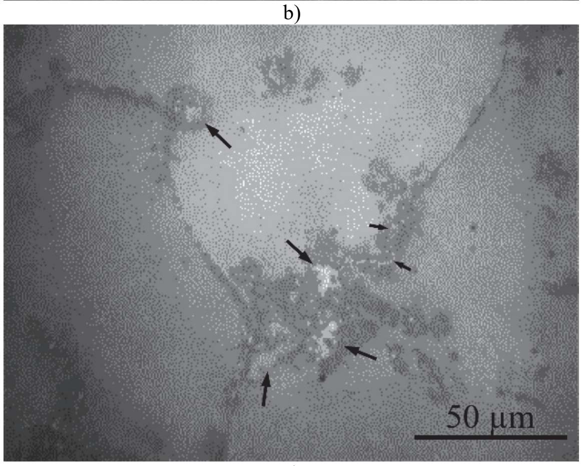

c)

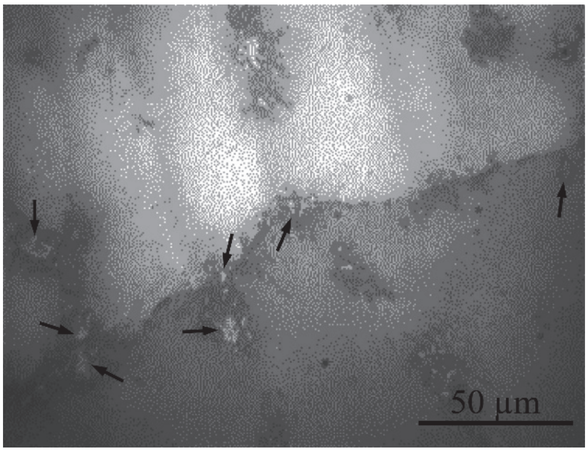

d)

Figure 5 Microstructure of Mn12 steel, WQA: a-b) sample (5); c-d) sample (6), magnification ×530, black arrows indicate carbides

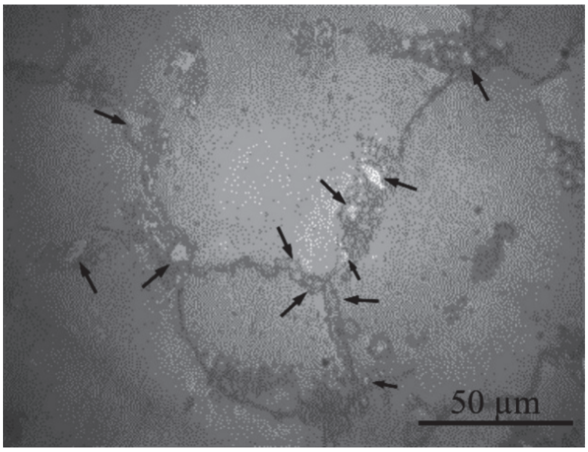

a)

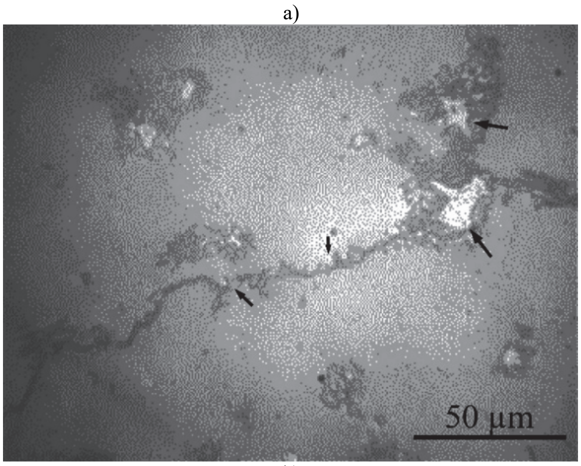

b)

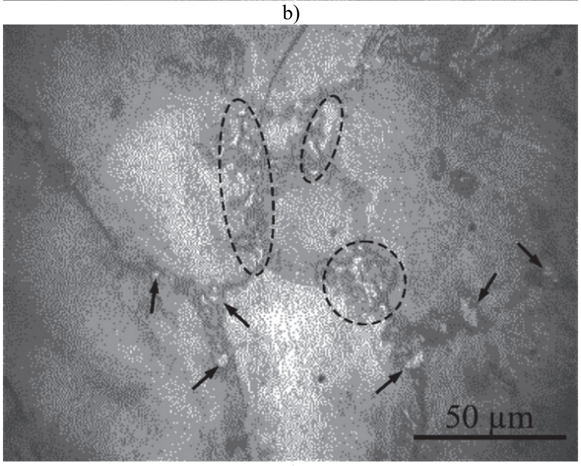

c)

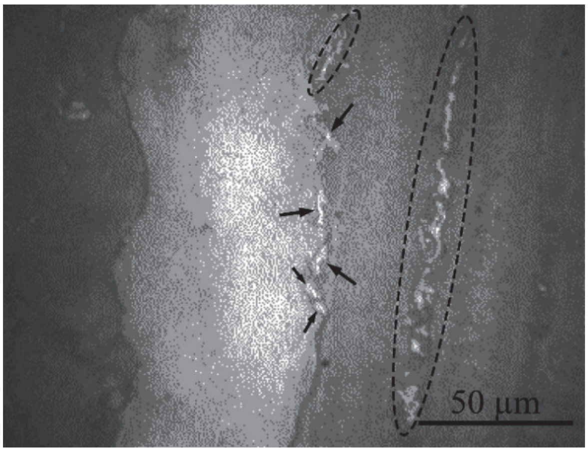

d)

Figure 6 Microstructure of Mn16 steel, WQA: a-b) sample (7); c-d) sample (8), magnification ×530, black arrows and dotted circles indicate carbides

The difference between Mn12 and Mn16 samples is attributed to variation in chemical composition. Addition of Mn enhances solid solution hardening, while increase of Cr and V will increase precipitation of carbides. On the other hand, due to increased supersaturation in Mn16 steels, nucleation of carbides on both grain boundaries and within austenite grains will be accelerated, resulting in smaller particles. Carbides in Mn12 steels are coarser and, less efficient [2, 3, 6]. More details can be found in [15], where these microstructures are also presented, but with different magnification.

3.2 Impact Toughness

Energies for crack initiation and propagation are obtained from diagrams force-time obtained on the instrumented Charpy pendulum. As example, diagrams force-time and energy-time for one specimen from samples (1) and (4) in WQ state are shown in Fig. 7.

Results for total energies and their separated values (crack initiation and propagation), as obtained on the instrumented Charpy pendulum, are shown in Tabs. 2a-2d for water quenched (WQ) samples (1)-(4), respectively, and in the same way in Tabs. 3a-3d for water quenched and aged (WQA) samples. Tab. 4 presents an overview of the mean values for crack initiation and propagation energy, as well as for the total energy to make comparison and analysis easier.

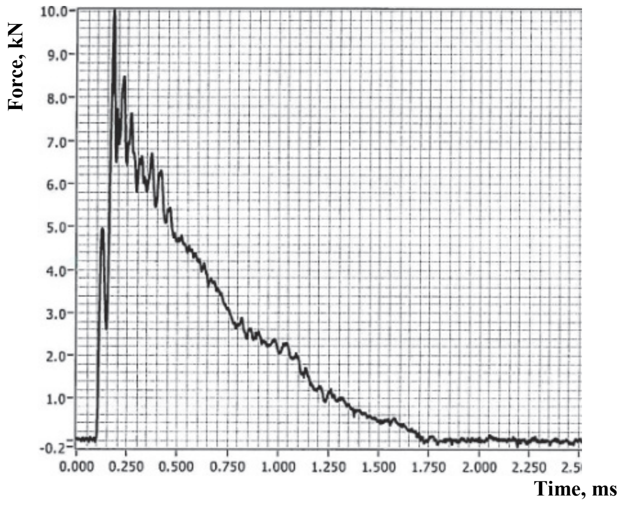

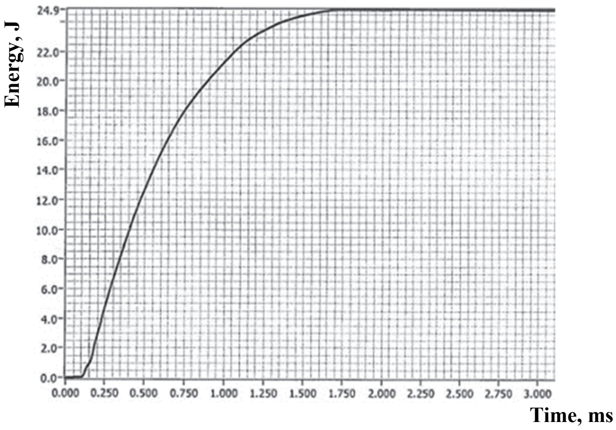

Figure 7 Force-time and energy-time diagrams for two WQ samples: a) sample (1), specimen 2; b) sample (4), specimen 4

Table 2a Energies E_i, E_p and E_t for WQ sample (1)

Specimen	E_i / J	E_p / J	E_t / J
1	6.6	15.2	21.8
2	6.2	17.0	23.2
3	4.5	19.8	24.3
Mean value	**5.8**	**17.3**	**23.1**

Table 2b Energies E_i, E_p and E_t for WQ sample (2)

Specimen	E_i / J	E_p / J	E_t / J
1	3.0	10.0	13.0
2	3.7	8.6	12.3
3	2.3	6.4	8.7
Mean value	**3.0**	**8.3**	**11.3**

Table 2c Energies E_i, E_p and E_t for WQ sample (3)

Specimen	E_i / J	E_p / J	E_t / J
1	4.6	25.8	30.4
2	6.6	26.4	33.0
3	15.4	32.8	48.2
Mean value	**8.8**	**28.4**	**37.2**

Table 2d Energies E_i, E_p and E_t for WQ sample (4)

Specimen	E_i / J	E_p / J	E_t / J
1	4.9	24.3	29.2
2	8.1	26.3	34.4
3	12.7	36.2	48.9
Mean value	**8.6**	**28.9**	**37.5**

Table 3a Energies E_i, E_p and E_t for WQA sample (1)

Specimen	E_i / J	E_p / J	E_t / J
1	12.2	20.7	33.0
2	6.0	22.4	28.4
3	8.2	22.5	30.7
Mean value	**9.1**	**21.6**	**30.7**

Table 3b Energies E_i, E_p and E_t for WQA sample (2)

Specimen	E_i / J	E_p / J	E_t / J
1	3.5	23.4	26.9
2	5.1	26.2	31.3
3	6.2	27.3	33.5
Mean value	**4.9**	**25.6**	**30.5**

Table 3c Energies E_i, E_p and E_t for WQA sample (3)

Specimen	E_i / J	E_p / J	E_t / J
1	3.8	20.9	24.4
2	7.5	20.7	28.2
3	2.0	16.7	18.7
Mean value	**4.4**	**19.4**	**23.8**

Table 3d Energies E_i, E_p and E_t for WQA sample (4)

Specimen	E_i / J	E_p / J	E_t / J
1	2.2	17.7	19.9
2	4.4	14.9	19.3
3	2.7	15.3	18.3
Mean value	**3.1**	**16.1**	**19.2**

Table 4 Crack initiation + propagation energy = total energy [J], mean values

Sample	$E_i + E_p = E_t$ (WQ)	Sample	$E_i + E_p = E_t$ (WQA)
(1)	5.8 + 17.3 = 23.1	(5)	9.1 + 21.6 = 30.7
(2)	3.0 + 8.3 = 11.3	(6)	4.9 + 25.6 = 30.5
(3)	8.8 + 28.4 = 37.2	(7)	4.4 + 19.4 = 23.8
(4)	8.6 + 28.9 = 37.5	(8)	3.1 + 16.1 = 19.2

From total energies values, Tab. 4, one can see that samples (1) and (2), i.e. steel Mn12, has higher toughness in WQA state, samples (5) and (6), contrary to samples (3) and (4), i.e. steel Mn16, has higher toughness in WQ state than in WQA state, samples (7) and (8). Generally speaking, toughness is just about sufficient in WQA state of steel Mn12 and in WQ state of steel Mn16. These results indicate that ageing did not produce considerably finer microstructure, i.e. it can be assumed that primary carbides present after quenching still played the dominant role in crack initiation, and respectively relatively low toughness.

One can also see that the crack initiation energies are significantly smaller than the crack propagation energies for all samples, indicating high sensitivity of tested steels to cracking and somewhat better resistance to crack propagation. This behavior can be attributed to the presence of austenite in microstructure, i.e. FCC lattice which has good plasticity.

4 CONCLUSIONS

The effect of composition and heat treatment on the impact toughness of Hadfield steel was investigated using two types of Hadfield steel, Mn12 and Mn16 and two heat treatments: WQ and WQA. The results show that Mn12 steels exhibit higher toughness after WQA, while Mn16 steels show higher toughness after WQ. Such a behaviour is attributed to the difference in the size and distribution of carbides. In Mn12 steels, the carbides are coarser and less efficient in hindering crack propagation, while in Mn16 steels, the carbides are finer and more effective in impeding crack.

Based on the results presented here, one can conclude the following:

- The effect of alloying on impact toughness of Hadfield steel is beneficial in the case of WQ, but not in the case of QWA.
- The effect of heat treatment on impact toughness of Hadfield steel is beneficial for Mn12 steels, but not for Mn16 steels.
- Both effects are important because they enable minimum total energy of 30 J in the case of WQ Mn16 and in the case of WQA Mn12 steel.
- Hadfield steel is more sensitive to crack initiation than to crack propagation under impact loading.

6 REFERENCES

[1] Hadfield, R. A. (1882). *Manufacturing of steel*, United States Patent No. 200, 05.08.1882, 303.

[2] Akeel, D. & Omar, A. (2007). Phase transformations of Hadfield manganese steels. *Engineering & Technology, 25*(26), 227-289. https://doi.org/10.30684/etj.25.6.9

[3] Dastur, Y. N. & Leslie, W. C. (1981). Mechanism of work hardening in Hadfield manganese steel. *Metallurgical Transactions A*, *12*(A), 749-758. https://doi.org/10.1007/BF02648339

[4] Drobnjak, Dj. & Parr, J. G. (1975). *Metallurgical Transactions*, *40*, 554.
[5] Chojecki, A. & Telejko, I. T. (2009). Cracks in high manganese cast steels. *Archives of Foundry Engineering*, *9*(4), 17-22.
[6] Mahlami, C. S. & Pan, X. (2017). Mechanical properties and microstructure evaluation of high manganese steel alloyed with vanadium. *AIP Conference Proceedings*, *1859*, 020083. https://doi.org/10.1063/1.4990236
[7] Lazić, V. et al. (2009). Reparation of the damaged forging hammer mallet by hard facing and weld cladding. *Tehnički vjesnik*, *16*(4), 107-113.
[8] Todić, A. et al. (2022). Influence of vanadium content on the tribological behaviour of X140CrMo12-1 air-hardening steel. *Transactions of FAMENA*, *46*(2), 15-22. https://doi.org/10.21278/TOF.462035021
[9] Youn-Soo, H. et al. (2010). Critical cooling rate on carbide precipitation during quenching of austenitic manganese steel. *China Foundry*, *7*(2), 177-182.
[10] Grabulov, V., Burzić, Z., & Momčilović, D. (2008). Significance of mechanical testing for structural integrity. *Proceedings of IFMASS 9*, 121-150.
[11] Perković, S., Radaković, Z., Burzić, Z., Sedmak, S., & Sedmak, A. (2023). Stress concentration effects on toughness value of duplex steel S32750. *Structural Integrity and Life*, *23*(1), 3-7.
[12] Perković, S. et al. (2025). Temperature and crack effects on impact toughness of S32750 steel welded joints. *Structural Integrity and Life*, *25*(1), 3-6.
[13] Jovanović, M., Camagić, I., Sedmak, S., Živković, P., & Sedmak, A. (2020). Crack initiation and propagation resistance of HSLA steel welded joint constituents. *Structural Integrity and Life*, *20*(1), 11-14.
[14] SRPSEN ISO 14556:2020. (2020). *Metallic materials - Charpy V-notch pendulum impact test - Instrumented test method.*
[15] Vukosavljević, A., Sedmak, A., Tadić, S., Radović, Lj., & Radović, N. (2025). Composition and heat treatment effects on hardness and strength of a Hadfield steel. *Structural Integrity and Life*, *25*(1), 7-10. https://doi.org/10.69644/ivk-2025-01-0011

Contact information:

Aleksandar VUKOSAVLJEVIĆ, PhD Student
University of Belgrade, Faculty of Technology and metallurgy,
Karnegijeva 4, 11000 Belgrade, Serbia
E-mail: vukalek@gmail.com

Aleksandar SEDMAK, PhD, Professor Emeritus
(Corresponding author)
University of Belgrade, Faculty of Mechanical Engineering,
Kraljice Marije 16, 11120 Belgrade, Serbia
E-mail: asedmak@mas.bg.ac.rs

Srđan TADIĆ, PhD, Scientific Associate
Innovation Center of Faculty of Mechanical Engineering,
Kraljice Marije 16, 11120 Belgrade, Serbia
E-mail: stadic@mas.bg.ac.rs

Srđa PERKOVIĆ, PhD, Scientific Associate
Military Technical Institute,
Ratka Resanovića 2, 11000 Belgrade, Serbia
E-mail: perkovic.srdja@gmail.com

Nenad RADOVIĆ, PhD, Full Professor
University of Belgrade, Faculty of Technology and metallurgy,
Karnegijeva 4, 11000 Belgrade, Serbia
E-mail: nenrad@tmf.bg.ac.rs